International Journal of Thermophysics, Vol. 19, No. 3, 1998

Thermophysical Properties of W–Re Alloys Above the Melting Region[1]

V. Didoukh,[2] A. Seifter,[3] G. Pottlacher,[3,4] and H. Jäger[3]

In earlier experiments we have studied pure elements with a fast pulse heating technique to obtain thermophysical properties of the liquid state. We report here results for thermophysical properties such as specific heat and dependences among enthalpy, electrical resistivity, and temperature, for four W–Re alloys (3.95, 21.03, 23.84, and 30.82 at % of Re) in a wide temperature range covering solid and liquid states. Thermal conductivity is calculated using the Wiedemann–Franz law for the liquid alloy, as well as data for thermal diffusivity for the beginning of the liquid phase. Additionally, data for the entire temperature range studied have been analyzed in comparison with those of the constituent elements, tungsten and rhenium, since both metals have been studied previously with the same experimental technique. Such information is of interest in the field of metallurgy since W–Re alloys of low Re content in the region of mutual component solubility in the solid state are widely used as thermocouple materials for the purposes of high-temperature thermometry.

KEY WORDS: electrical resistivity; enthalpy; high temperature; liquid alloys; rhenium alloy; specific heat; thermal conductivity; thermal diffusivity; tungsten alloy.

1. INTRODUCTION

Fast dynamic pulse-heating methods have been developed to extend measurements to extremely high temperatures by heating up the specimen in a

[1] Paper presented at the Thirteenth Symposium on Thermophysical Properties, June 22–27, 1997, Boulder, Colorado, U.S.A.

[2] Institute of Applied Physics, Ivan Franko State University, Pushkin Street 49, 290044 Lviv, Ukraine.

[3] Institute für Experimentalphysik, Technische Universität Graz, Petersgasse 16, A-8010 Graz, Austria.

[4] To whom correspondence should be addressed.

0195-928X/98/0500-0969$15.00/0

very short time into the liquid state while the sample maintains its initial geometrical shape because of inertia [1, 2]. Since most metals and their alloys can be produced in wire-shaped form of appropriate dimensions, pulse heating techniques are found to be measuring methods of general importance for the investigation of thermophysical properties of electrically conducting solids and fluids. Using this method, refractory metals like tungsten and rhenium have been intensively studied during the last few decades [3–10] and the properties for almost all these metals in solid and liquid states were determined with rather good precision. However, properties of alloys of refractory metals, despite the prospects of their practical application, still remain less known up to now. Practically, there are no systematic data for the thermophysical properties of these alloys in the liquid state. In best cases, the information is available only for the solid state [11–14].

Tungsten and rhenium have the highest melting temperatures among the metals, i.e., 3695 and 3453 K, respectively. The phase diagram of the binary W–Re alloy system presented in a handbook [15] is based mainly on the results of Ref. 16, except for the solidus of the terminal phases, which are taken from Ref. 17. In the solid state, the solubility of Re in W is equal to 37 at % at 3273 K according to Ref. 16 or even up to 45 at % at 3163 K as reported in Ref. 17.

To the best of our knowledge, the properties of solid and especially of liquid W–Re alloys in the concentration range of continuous solid Re in W solutions are reported for the first time. The information is of interest in the field of refractory metals metallurgy, since such alloys are widely used as thermoelectrode materials for the purposes of high temperature thermometry.

2. EXPERIMENTAL PROCEDURE

Wire-shaped W–Re alloy specimens are resistively volume heated into the liquid phase by passing a large current pulse through them. Heating rates of about 10^8 K · s^{-1} were achieved. The measurements were performed in air at atmospheric pressure. More details on the experiment and on the data reduction are given elsewhere [18].

In contrast to pure metals, alloys have a certain melting region instead of a constant melting temperature. The absence of a clearly detectable melting point, as well as the possible variation of the surface radiation intensity within the melting region, complicates the proper choice of a reference temperature. Therefore, in the present work, for each of the investigated alloys, an averaged value of respective solidus and liquidus temperatures from the phase diagram was adopted as the reference melting temperature for

Table I. Parameter of Wire Samples; Density Values Are Calculated Assuming that Each Component Contributes to the Sample Density in Proportion to Its Percentage Weight in the Alloy

Sample	Conc. at % of Re	Weight % of Re	Density ($kg \cdot m^{-3}$)	$T_{ref.}$ (K)	Diameter (mm)
N1	3.95	4.00	19.362	3618	0.35
N2	21.03	21.24	19.637	3423	0.35
N3	23.84	24.07	19.683	3398	0.35
N4	30.82	31.09	19.798	3358	0.50
W			19.300	3683	
Re			21.000	3180	

the experimental data analysis, as is discussed in Section 3. These values together with density, chemical composition, and diameter of the wire samples are given in Table I for each alloy studied.

The thermal conductivity λ may be evaluated from electrical resistivity ρ by the Wiedemann–Franz law,

$$\lambda = LT/\rho \tag{1}$$

L is the Lorenz number ($2.45 \times 10^{-8}\ V^2 \cdot K^2$) and T is the temperature of the specimen. As discussed in Ref. 19, the principal carriers for the thermal conduction in solid metals are electrons and lattice waves. However, for temperatures close to the melting point of pure metals, electronic conduction is the predominant mechanism and lattice conduction is negligible. The Lorenz number L for most pure metals is close to its theoretical value. In this way, Eq. (2) is a good tool to obtain thermal conductivity in the vicinity of the melting point. Furthermore, it is also possible to evaluate the thermal diffusivity a, which is related to the thermal conductivity λ, specific heat C_p, and density d of the material by

$$a = \lambda/(C_p d) \tag{2}$$

3. RESULTS

Figure 1 illustrates the temperature dependences of enthalpy measured in one single experiment for the sample N4 but calculated for three values of the reference temperature $T_{ref.}$, namely, H_1 for $T_{sol.}$, H_3 for $T_{liq.}$, and H_2 for $T_{ref.} = (T_{sol.} + T_{liq.})/2$, where $T_{sol.}$ and $T_{liq.}$ were taken from the phase diagram [15]. Temperatures are calculated with the help of Planck's law.

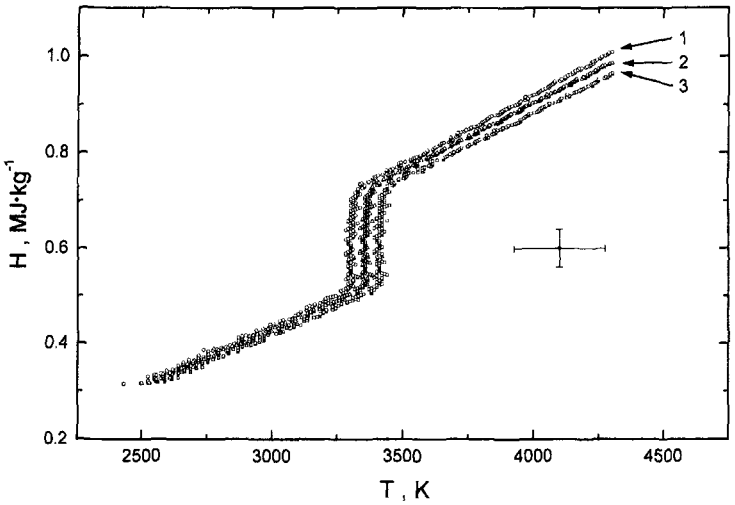

Fig. 1. Temperature dependences of enthalpy measured in one single experiment for the sample N4, analyzed for three values of the reference temperature: (1) $T_{\text{sol.}}$; (2) $(T_{\text{sol.}} + T_{\text{liq.}})/2$; (3) $T_{\text{liq.}}$.

The heat of fusion seems to be insensitive to a variation of the reference temperature between $T_{\text{sol.}}$ and $T_{\text{liq.}}$. The enthalpy in liquid and solid states increases almost linearly with temperature. This dependence may be described by a linear least-squares fit, and its slope yields a constant specific heat value. Because of the lack of sharp discontinuities at the beginning and at the end of the melting region, those data points, which lie in the transition between premelting and the plateau, and postmelting and the plateau, were excluded from the data fits.

In this way, we have obtained in Fig. 1 for the same material three values 292.2, 280.4, and 270.4 $\text{J} \cdot \text{kg}^{-1} \cdot \text{K}^{-1}$ of the specific heat in the liquid for the three reference temperatures $T_{\text{sol.}}$, $(T_{\text{sol.}} + T_{\text{liq.}})/2$, and $T_{\text{liq.}}$. The difference between the maximum and the minimum values does not exceed 8%. Up to 15% uncertainty in specific heat values in pulse heating experiments has to be assumed. Therefore, temperatures averaged between respective solidus and liquidus points of each alloy concentration $(T_{\text{sol.}} + T_{\text{liq.}})/2$ were taken as references for the analysis of the measured data. These temperatures are listed in Table I.

Figure 2 presents the enthalpy as a function of temperature for sample N4. During the melting transition, the enthalpy changes from $H_s = 0.516\ \text{MJ} \cdot \text{kg}^{-1}$ to $H_l = 0.734\ \text{MJ} \cdot \text{kg}^{-1}$, yielding $\Delta H = 0.218\ \text{MJ} \cdot \text{kg}^{-1}$ for the latent heat of fusion. The dependence of enthalpy on temperature for

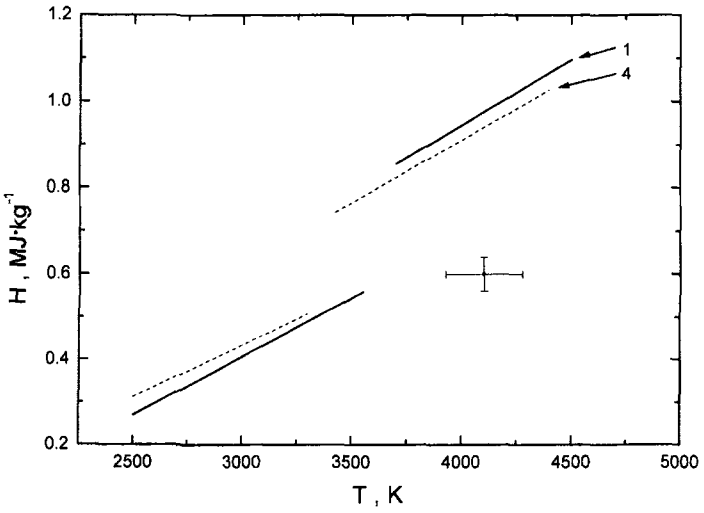

Fig. 2. Enthalpy as a function of temperature for sample N1 and N4, in the form of least-squares fits.

solid and liquid states is given by the following expressions, where H is in $\mathrm{MJ \cdot kg^{-1}}$ and T is in K:

$$H = -0.29388 + 0.2429 \times 10^{-3} T \quad \text{in the range} \quad 2500 < T < 3300 \tag{3}$$

$$H = -0.24507 + 0.2893 \times 10^{-3} T \quad \text{in the range} \quad 3430 < T < 4400 \tag{4}$$

The derivative of the linear regressions gives $C_p = 243\ \mathrm{J \cdot kg^{-1} \cdot K^{-1}}$ and $C_p = 289\ \mathrm{J \cdot kg^{-1} \cdot K^{-1}}$ for the specific heat of the alloy N4 in solid and liquid states, respectively.

The least-squares fits which summarize measured $H(T)$ dependences for the other alloys investigated are given below. The values for N1 and N4 are illustrated in Fig. 2; N2 and N3 are not given in Fig. 2, as they are between the values of N1 and N4.

Alloy N3:

$$H = -0.30285 + 0.2443 \times 10^{-3} T \quad \text{in the range} \quad 2500 < T < 3300 \tag{5}$$

$$H = -0.24523 + 0.2902 \times 10^{-3} T \quad \text{in the range} \quad 3490 < T < 4400 \tag{6}$$

Alloy N2:

$$H = -0.34065 + 0.2556 \times 10^{-3} T \quad \text{in the range} \quad 2500 < T < 3340 \tag{7}$$

$$H = -0.23415 + 0.2911 \times 10^{-3} T \quad \text{in the range} \quad 3510 < T < 4400 \tag{8}$$

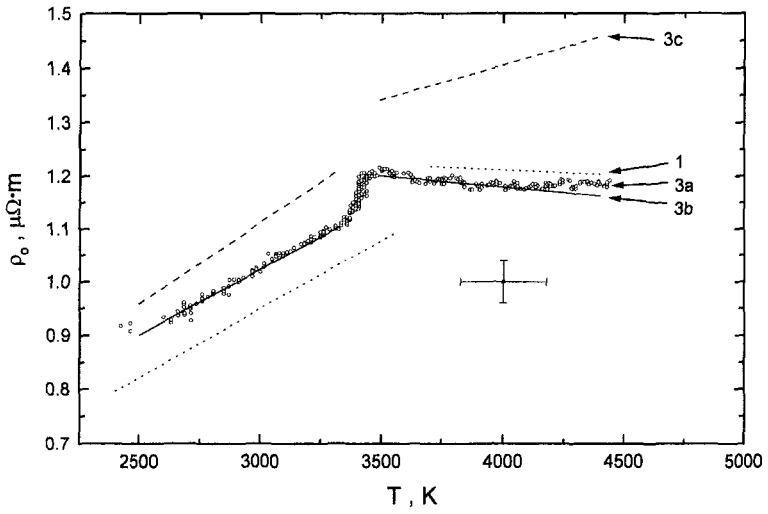

Fig. 3. Electrical resistivity of the alloy N3, least-squares fit for ρ (corrected for thermal expansion; c), and least-squares fit ρ_0 (not corrected; b) as a function of temperature. (a) Results of a single measurement. Electrical resistivity ρ_0 (not corrected; 1) of alloy N1 as a function of temperature in form of least-squares fits.

Alloy N1:

$$H = -0.41911 + 0.2756 \times 10^{-3} T \quad \text{in the range} \quad 2900 < T < 3550 \tag{9}$$

$$H = -0.26164 + 0.3020 \times 10^{-3} T \quad \text{in the range} \quad 3700 < T < 4500 \tag{10}$$

Figure 3 presents the electrical resistivity of alloy N3 [ρ_0, not corrected (3b); ρ, corrected for thermal expansion (3c)] as a function of temperature using least-squares fits. The results of a single typical measurement are given as open circles (3a). Electrical resistivity ρ_0 of alloy N1 as a function of temperature is also given in Fig. 3. The determined dependences may be described by the following expressions for uncorrected resistivity ρ_0 in $\mu\Omega \cdot$ m and T in K.

Alloy N3:

$$\rho_0 = 2.9045 \times 10^{-1} + 2.44 \times 10^{-4} T$$
$$\text{in the range} \quad 2500 < T < 3320 \tag{11}$$

$$\rho_0 = 1.351194 - 4.28743 \times 10^{-5} T$$
$$\text{in the range} \quad 3490 < T < 4400 \tag{12}$$

For volume corrected resistivity (ρ in $\mu\Omega \cdot$ m, T in K) the relations are as follows.

Alloy N3:

$$\rho = 1.8963 \times 10^{-1} + 3.07733 \times 10^{-4} T \quad \text{in the range } 2500 < T < 3320 \tag{13}$$

$$\rho = 8.999 \times 10^{-1} + 1.26691 \times 10^{-4} T \quad \text{in the range } 3490 < T < 4400 \tag{14}$$

which is for the solid and the liquid states.

The other W–Re alloys investigated in this work show a very similar temperature behavior of noncorrected resistivity, i.e., increasing in the solid state and decreasing in the liquid state. By means of least-squares fits, the following $\rho_0(T)$ dependences were obtained from a large number of experimental data points.

Alloy N1:

$$\rho_0 = 1.79186 \times 10^{-1} + 2.57 \times 10^{-4} T$$

$$\text{for the range } 2900 < T < 3550 \tag{15}$$

$$\rho_0 = 1.298049 - 2.15784 \times 10^{-5} T$$

$$\text{for the range } 3700 < T < 4400 \tag{16}$$

Alloy 2:

$$\rho_0 = 2.94835 \times 10^{-1} + 2.48 \times 10^{-4} T$$

$$\text{for the range } 2500 < T < 3340 \tag{17}$$

$$\rho_0 = 1.439627 - 5.82841 \times 10^{-5} T$$

$$\text{for the range } 3510 < T < 4400 \tag{18}$$

Alloy 4:

$$\rho_0 = 2.56844 \times 10^{-1} + 2.65 \times 10^{-4} T$$

$$\text{for the range } 2500 < T < 3300 \tag{19}$$

$$\rho_0 = 1.410894 - 5.0112 \times 10^{-5} T$$

$$\text{for the range } 3430 < T < 4400 \tag{20}$$

The fits for N2 and N4 are again very close to the other plots and therefore not shown in Fig. 3.

The set of experimentally determined properties can be used with Eqs. (1) and (2) to calculate the temperature behaviors of the thermal conductivity λ and thermal diffusivity a. As an example, Fig. 4 shows the results of such an estimation for alloy N3. The values of these properties, and their

dependences on temperature can be described (λ is in $W \cdot K^{-1} \cdot m^{-1}$ and a in $m^2 \cdot s^{-1}$) by

$$\lambda = 5.38725 \times 10^1 + 3.9995 \times 10^{-3} T$$
$$\text{in the range} \quad 2500 < T < 3320 \tag{21}$$
$$\lambda = 2.43702 \times 10^1 + 1.13 \times 10^{-2} T$$
$$\text{in the range} \quad 3490 < T < 4400 \tag{22}$$

and

$$a = 1.04124 \times 10^{-5} + 1.49329 \times 10^{-9} T$$
$$\text{in the range} \quad 2500 < T < 3320 \tag{23}$$
$$a = -0.20218 \times 10^{-5} + 4.1489 \times 10^{-9} T$$
$$\text{in the range} \quad 3490 < T < 4400 \tag{24}$$

which is for the solid and the liquid states.

The values of the specific heat of the W–Re alloys in solid and liquid states, their melting enthalpies, enthalpies, and uncorrected electrical resistivity values at the beginning and at the end of melting, compared with results for pure tungsten and rhenium, are summarized in Table II.

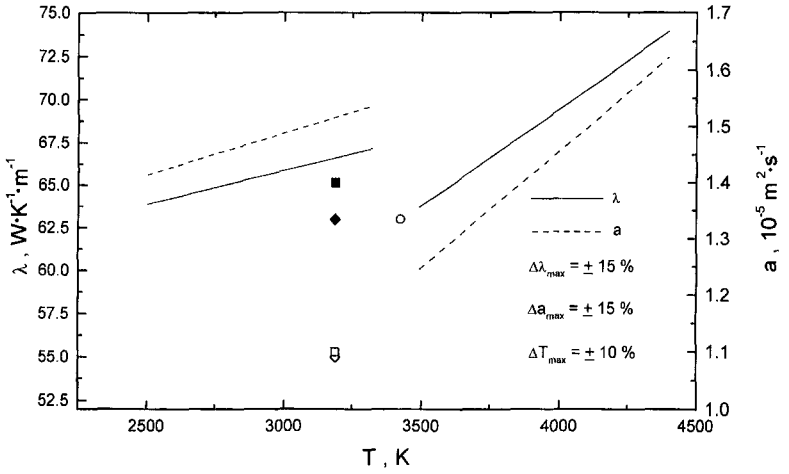

Fig. 4. Thermal conductivity λ (solid line) and thermal diffusivity a (dashed line) as a function of temperature for the alloy N3. Reference values from Ref. 19 for solid (filled figures) and liquid (open figures) rhenium (λ, diamonds; a squares) and for liquid tungsten (λ, open circle) are also indicated.

Table II. Values of Specific Heat of the W–Re Alloys in Solid and Liquid States, Melting Enthalpies, and Uncorrected Electrical Resistivity Values at the Beginning and at the End of Melting (ρ_0), Compared with Literature Data of Tungsten and Rhenium (Volume Corrected Values ρ)

Sample	Ref.	H_s ($MJ \cdot kg^{-1}$)	H_l ($MJ \cdot kg^{-1}$)	ΔH ($MJ \cdot kg^{-1}$)	ρ_s ($\mu\Omega \cdot m$)	ρ_l ($\mu\Omega \cdot m$)	$C_{p(sol)}$ ($\mu\Omega \cdot m$)	$C_{p(liq)}$ ($J \cdot kg^{-1} \cdot K^{-1}$)	$C_{p(calc)}$ ($J \cdot kg^{-1} \cdot K^{-1}$)
Alloy N1	this work	0.568	0.827	0.259	$1.11(\rho_0)$	$1.23(\rho_0)$	276	302	303
Alloy N2	this work	0.529	0.763	0.234	$1.15(\rho_0)$	$1.24(\rho_0)$	256	291	293
Alloy N3	this work	0.524	0.750	0.226	$1.12(\rho_0)$	$1.23(\rho_0)$	244	290	292
Alloy N4	this work	0.516	0.734	0.218	$1.14(\rho_0)$	$1.24(\rho_0)$	243	289	288
Re	[4]	0.520	0.670	0.150	$1.20(\rho)$	$1.37(\rho)$		250	
	[3]	0.615	0.768	0.153	$1.451(\rho)$	$1.457(\rho)$	226	267	
	[10]							225	
	[5]	0.577	0.735	0.158	$1.180(\rho)$	$1.188(\rho)$	180	233	
W	[6]	0.629	0.885	0.256	$1.179(\rho)$	$1.38(\rho)$		305	
	[9]	0.617	0.881	0.264	$1.20(\rho)$	$1.35(\rho)$		310	
	[8]	0.610	0.870	0.260	$1.26(\rho)$	$1.46(\rho)$		262	
	[7]	0.616	0.870	0.254	$1.23(\rho)$	$1.38(\rho)$		300	

4. ESTIMATE OF UNCERTAINTIES

Enthalpy is the most accurate of all the properties measured, with an estimated uncertainty of $\pm 4\%$. For the temperature measurements the uncertainty is $\pm 5\%$ in the melting region, increasing to about $\pm 10\%$ in the liquid phase. The uncertainty in the uncorrected electrical resistivity is estimated to be $\pm 4\%$, increasing to $\pm 7\%$ for the corrected electrical resistivity. An uncertainty of $\pm 5\%$ is estimated for the density in the solid phase, increasing for the lowest densities in the liquid phase up to $\pm 10\%$. The estimated uncertainty in the melting enthalpy is $\pm 5\%$, in the specific heat about $\pm 15\%$, and in thermal conductivity and thermal diffusivity about $\pm 15\%$. The individual error bars are indicated in each figure.

5. DISCUSSION

As can be seen from the data in Table II, the investigated W–Re alloys have enthalpy values at the beginning and the end of melting comparable with those of pure W and Re (see Fig. 5). For each alloy the enthalpy at the end of melting does not exceed the respective value of pure tungsten

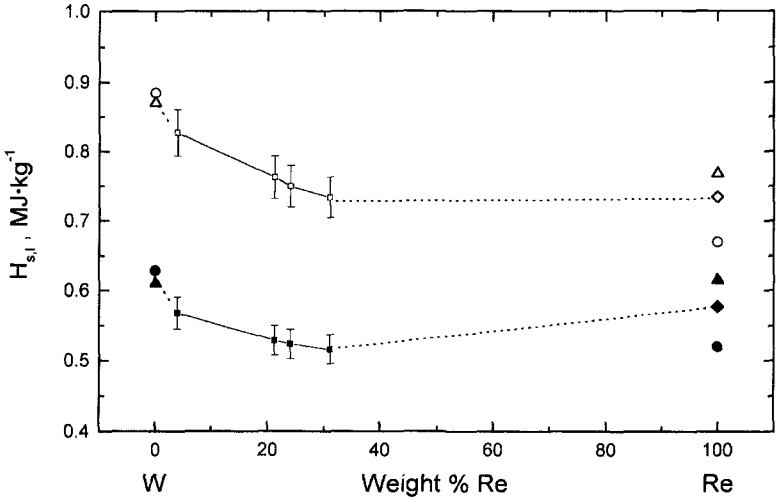

Fig. 5. Enthalpy values at the beginning (small filled squares) and the end of melting (small open squares) for different weight % Re, compared to those of pure W and Re. Filled symbols indicate the beginning, and open symbols indicate the end of melting. Triangles: Hixson and Winkler [3] for Re and Hixson and Winkler [8] for W. Circles: Kaschnitz et al. [6] for W and Pottlacher et al. [4] for Re. Diamonds: Thevenin et al. [5] for Re. The values of Berthault et al. [7] for W cannot be indicated here, as they would overlap the W values [8].

and decreases continuously with increasing Re contamination, as expected. The enthalpy at the beginning of melting shows the same concentration dependence, but the absolute values are lower than those for rhenium [3, 5] and are very close (with the exception of the alloy N1) to the H_s value reported in Ref. 4. However, even in this case the enthalpy at the beginning of melting of the alloy with the highest Re content (N4; $H_s = 0.516$ MJ · kg^{-1}) is slightly lower than the lowest value of 0.520 MJ · kg^{-1} reported for pure rhenium in [4]. Since enthalpy is a linear function of temperature, the H_S dependence on the component concentration reflects the shape of the solidus line on the phase diagram. The minimal H_s value for sample 4 evidently shows that its solidus temperature is lower than the melting point of pure rhenium, and Fig. 5 may be considered as a part of the W–Re phase diagram in the enthalpy–concentration plane.

Such diagrams give important additional information for purposes of metallurgy, especially for high-melting alloys in the region of their solid–liquid transition. In the case of W–Re alloys, the solidus and liquidus curves were not measured but, rather, estimated. We have found no information about exact melting temperatures for W–Re alloys containing less than 38 wt% Re in the literature [16, 17]. To the best of our knowledge, the solidus temperature was measured for only one W–Re alloy (3.24 wt% Re) by means of a fast dynamic technique [11]. The value reported (3645 K) is higher than the reference temperature adopted in our evaluation for an alloy of 4 wt% Re (see Table I). The absence of measured solidus and liquidus temperatures, which results in an increased uncertainty in the choice of the reference temperature, should be always taken into account when considering the results given above. However, the uncorrected resistivity for all W–Re alloys in the liquid state is a decreasing function of the temperature. This may be caused by an influence of rhenium, which demonstrates the same behavior [4, 5]. Volume-corrected resistivity shows a temperature dependence typical for metals (see Fig. 3) with slightly increasing resistivity with temperature.

To the best of our knowledge, measurements of the heat of fusion of W–Re alloys as well as their heat capacities in the liquid state have never been performed before. Consequently, there are no data for comparison. However, following the procedure used in Ref. 20, an estimated value for each alloy can be computed from values of the heat of fusion of the constituent metals in the alloy, assuming that each metal contributes to the total heat of fusion in proportion to its percent weight in the alloy. The computations were performed using the values for heat of fusion of tungsten, 0.256 MJ · kg^{-1} [6], and rhenium, 0.150 MJ · kg^{-1} [4], being measured previously with the same experimental technique. The computed values are 251.7, 233.5, 230.5, and 223 MJ · kg^{-1} for the alloys N1, N2, N3,

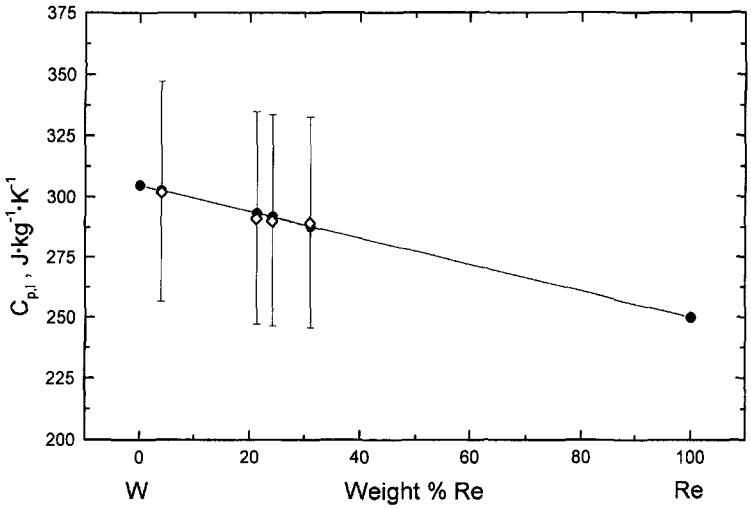

Fig. 6. Calculated C_p values (filled circles) and experimental values (open diamonds).

and N4, respectively. The experimentally determined values are in good agreement with these estimates.

The same relationship for the specific heat of alloys in the liquid state is well known from Kopp's law [21]. The calculations were performed based on the C_p values for liquid tungsten and rhenium obtained previously using the same pulse-heating technique [4, 6]. As can be seen from Table II and Fig. 6, the calculated C_p values according to the percentage weight for all investigated W–Re alloys agree within experimental error with those derived from the $H(T)$ diagrams. Since these experiments were performed for alloys in the concentration range of solid solutions [15], it can be suggested that this rule also might be valid for other high-melting binary alloys for the respective regions of their phase diagrams. Systematic investigations of the Ni–Fe system with this fast pulse heating technique [22] demonstrate the same behavior.

ACKNOWLEDGMENTS

One of us (V.D.) would like to thank the Technical University of Graz for a research fellowship. We also thank Dr. P. Golob from the Forschungsinstitut für Elektronenmikroskopie und Feinstrukturforschung, Graz for determination of sample compositions by means of EDAX.

REFERENCES

1. A. Cezairliyan, in *Compendium of Thermophysical Property Measurements Methods, Vol. 1*, K. D. Maglic, A. Cezairliyan, and V. E. Peletsky, eds. (Plenum Press, New York, 1984), pp. 643–668.
2. G. Pottlacher, in *Advances in Materials Science and Engineering, Third Supplement*, R. W. Cahn, ed. (Pergamon Press, Oxford, 1993), pp. 2056–2063.
3. R. S. Hixson and M. A. Winkler, *Int. J. Thermophys.* **13**:477 (1992).
4. G. Pottlacher, T. Neger, and H. Jäger, *Int. J. Thermophys.* **7**:149 (1986).
5. Th. Thevenin, L. Arles, M. Boivineau, and J. M. Vermeulen, *Int. J. Thermophys.* **14**:441 (1993).
6. E. Kaschnitz, G. Pottlacher, and L. Windholz, *High Press. Res.* **4**:558 (1990).
7. A. Berthault, L. Arles, and J. Matricon, *Int. J. Thermophys.* **7**(1):167 (1986).
8. R. S. Hixson and M. A. Winkler, *Int. J. Thermophys.* **11**(4):709 (1990).
9. U. Seydel, W. Fucke, and H. Wadle, *Die Bestimmung thermophysikalischer Daten flüssiger hochschmelzender Metalle mit schnellen Pulsaufheizexperimenten* (P. Mannhold, Düsseldorf, 1980).
10. R. Hultgren, P. D. Desai, D. T. Hawkins, M. Gleiser, K. K. Kelley, and D. D. Wagman, *Selected Values of the Thermodynamic Properties of the Elements* (Am. Soc. Metals, 1973).
11. A. Cezairliyan and A. P. Miiller, *Int. J. Thermophys.* **6**:191 (1985).
12. K. S. Sukhovei, *Soviet Phys. Solid State* **9**:2893 (1968).
13. Ya. A. Kraftmakher and A. G. Cherevko, *High Temp. High Press.* **7**:283 (1975).
14. A. V. Logunov and A. I. Kovalev, *High Temp. High Press.* **5**:625 (1973).
15. T. B. Massalski, P. R. Subramanian, H. Okamoto, and L. Kacprzak, *Binary Alloy Phase Diagrams*, 2nd ed. (ASM International, Materials Park, OH, 1990).
16. J. W. Dickinson and L. S. Richardson, *Trans. ASM* **51**:758 (1959).
17. E. M. Savitskii, M. A. Tylkina, and L. L. Shishkina, *Izv. Akad. Nauk SSSR Otd. Tekhn. Nauk Met. Toplivo* **3**:99 (1959).
18. E. Kaschnitz, G. Pottlacher, and H. Jäger, *Int. J. Thermophys.* **13**:699 (1992).
19. K. C. Mills, B. J. Monaghan, and B. J. Keene, NPL Report CMMT(A)53 (1997).
20. J. L. McClure and A. Cezairliyan, *Int. J. Thermophys.* **13**:75 (1992).
21. A. Cezairliyan, *J. Chem. Thermodyn.* **6**:735 (1974).
22. A. Seifter, Diploma thesis (Technische Universität Graz, 1996).